PERGAMON

Electrochimica Acta 46 (2000) 349–356

ELECTROCHIMICA Acta

www.elsevier.nl/locate/electacta

Recovery of Cu, Pb, Cd and Zn from synthetic mixture by selective electrodeposition in chloride solution

L. Doulakas [a], K. Novy [a], S. Stucki [b], Ch. Comninellis [a,*]

[a] *Institute of Chemical Engineering, Swiss Federal Institute of Technology, CH-1015 Lausanne, Switzerland*
[b] *Paul Scherrer Institute, CH-5232 Villigen, PSI Villigen, Switzerland*

Received 20 October 1999

Abstract

Secondary fly ash, resulting from thermal treatment processes, leads to a highly concentrated chloride solution with Cu, Pb, Cd and Zn as main heavy metals when dissolved in water. The selective electrodeposition of these heavy metals has been studied in this work. The goal was to recover, under potentiostatic conditions, each heavy metal with high purity, yield and reaction rates. By changing the parameters pH and overpotential, an optimum of the three requirements was looked for. In general, Cu, Pb and Cd could be separated with purities of 99 mol% or higher. Underpotential deposition was supposed to be the main reason for the impurities in case of Cu and Pb deposition. H^+ reduction as side reaction could be kept small for Cu, Pb and Cd even at lower pH by carefully selecting the overpotential. The quality of the deposits obtained depended strongly on the overpotential, but hardly on the pH. The deposits of Cu, Pb and Cd were easily removable from the cathode due to a dendritic growth mechanism. Zn deposits showed compact growth and adhered to the electrode surface. In addition, the structure of the deposits, revealed by scanning electron microscope (SEM), was compared with the current transients during electrodeposition. An enhancement factor r was introduced in order to compare the different deposition rates.

Keywords: Heavy metals; Selective recovery; Chlorides; Electrodeposition; Potentiostatic control

1. Introduction

Electrodeposition has been usually applied for the recovery of metals from wastewater or for electroplating. In general, only one metal cation is present in the solution. Possible cathodic side reactions are H_2 evolution and reduction of the dissolved O_2 to H_2O, which may affect the current efficiency but not the purity of the deposit. In general, these processes are carried out under galvanostatic conditions using two- or three-dimensional electrodes. A lot of research has been carried out with solutions containing only one metal studying the effect of different anions. Harrison [1] determined the rate of deposition of Cu, Zn and Cd in solutions containing SO_4^{2-}, Cl^-, ClO_4^- or PO_4^{3-}. Fontana et al. [2] investigated the electrodeposition of Cu from pure cupric chloride in hydrochloric acid solution. For Pb, Kuhn [5] did not mention specific problems for the electrodeposition of lead from chloride containing solutions. The kinetics of Cd reduction on Hg in Cl^- containing solutions was determined [3]. For Zn, Hsie et al. [4,5] investigated the mass transport in supported zinc halide solutions. Scou et al. [6] made calculations about the metal–chloride complex formation using zinc as an example.

* Corresponding author. Tel./fax: +41-21-6933674.
E-mail address: christos.comninellis@epfl.ch (C. Comninellis).

0013-4686/00/$ - see front matter
PII: S0013-4686(00)00591-0

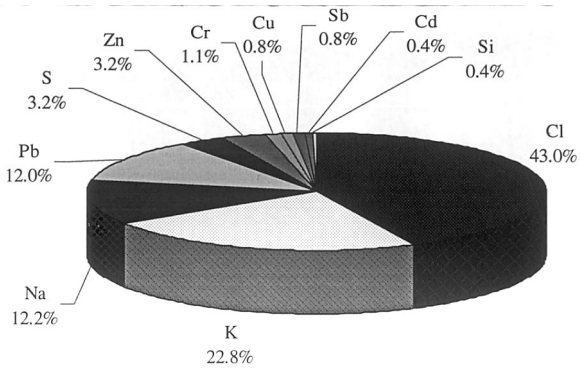

Fig. 1. Main composition of the Deglor secondary fly ash as mass% from the total.

Less research was carried out in the field of selective separation of metal cations from solutions containing two or more metal cations. The process becomes more complicated as there is a possibility of simultaneous discharge of several cations leading to a decreased deposit purity. In this case, the electrodeposition should be carried out under potentiostatic control. Suzuki et al. [7] investigated binary and ternary mixtures Ag/Cu/Zn and Cu/Cd/Zn from metal plating wastes. Non-complexing solutions containing SO_4^{2-} and NO_3^- were used as well as complexing solutions as citrate Na_3 or tartrate KNa. Wang et al. [8] used an RVC electrode to remove single metal ions from diluted solutions and binary mixtures of copper and lead. Armstrong et al. [9] investigated electroseparation of Co and Ni from a simulated wastewater.

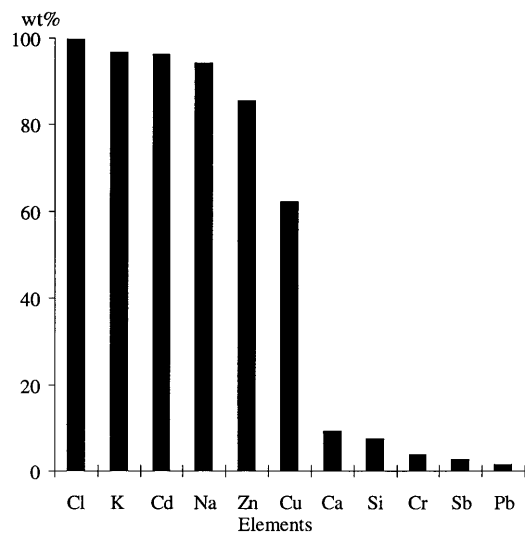

Fig. 2. Concentration of elements in the filtrate (black) expressed as percentage of the total amount in the Deglor secondary fly ash.

In this paper, the selective deposition is reported on under potentiostatic conditions from concentrated chloride solutions containing Cu(II), Pb(II), Cd(II), Zn(II) as heavy metals. The aim of this work is the application of this technology to the selective recovery of these metals from secondary fly ashes produced by thermal treatment methods [10] of fly ash. The secondary fly ash of the ABB Deglor® process [11]) was chosen as example.

2. Experimental features

In Fig. 1, the composition of the secondary fly ash resulting from the ABB Deglor® process is shown. For further information concerning the physical and chemical properties see Ref. [11]. After adding 1 g of Deglor secondary fly ash to an excess (10 ml) of deionised water and filtration using a filter with a porosity of 17–40 μm, a filtrate and a precipitate were obtained. The filtrate contains about 85 wt.% of the initial material. In Fig. 2, the concentration of the elements in the filtrate expressed as a percentage of the total amount in the Deglor condensate is shown. The most important cationic components in the filtrate were Na, K, Zn, Cu, Pb and Cd. Although $PbCl_2$ is quite insoluble (K_s = 4.77), its concentration in the soluble phase is similar to the concentration of copper or cadmium. The pH of the filtrate was around 6. To avoid precipitation of hydroxides, the pH was decreased by adding HCl (Fluka HCl conc. 32%). In order to have well defined initial conditions for electrochemical investigations, a standard solution was prepared having a composition similar to the filtrate. The standard solution was made up with 2.53 g $ZnCl_2$ (Merck pur), 0.43 g $PbCl_2$ (Fluka > 99%), 0.5g $CuCl_2$ (Fluka > 97%), 0.27 g $CdCl_2$ (Siegfried pur: 99.8%), 14.55 g NaCl (Fluka > 99.5%), and 19.9 g KCl (Fluka > 99%) in 100 ml of water, acidified with HCl to either pH 1.5 or 3.5. This leads to the following concentrations: Zn^{2+} = 0.172 M, Pb^{2+} = 0.0154 M, Cu^{2+} = 0.035 M, Cd^{2+} = 0.0149 M, Na^+ = 2.48 M, K^+ = 2.66 M and Cl^- = 5.6 M.

To investigate the separation of copper, lead, cadmium and zinc by electrochemical deposition, four synthetic solutions A, B, C and D based on the standard solution have been prepared, see Table 1. All experiments were performed at room temperature (24°C ± 2°C) and normal atmospheric pressure.

A batch reactor, shown in Fig. 3, containing three electrodes was used as experimental cell. The solution volume was 40 ml. The applied potential, supplied by the potentiostat EG&G Model 362, was constant with respect to the reference electrode, a saturated calomel electrode (Tacussel XR110). All potentials are expressed versus SCE. The anode was a platinum wire, separated from the two other electrodes by a glass frit

Table 1
Composition of the four synthetic solutions used (M)

Solution	$CuCl_2$	$PbCl_2$	$CdCl_2$	$ZnCl_2$	KCl	NaCl	pH
A	0.035	0.0154	0.0149	0.172	2.66	2.48	1.5
B		0.0154	0.0149	0.172	2.66	2.48	1.5 or 3.5
C			0.0149	0.172	2.66	2.48	1.5 or 3.5
D				0.172	2.66	2.48	3.5

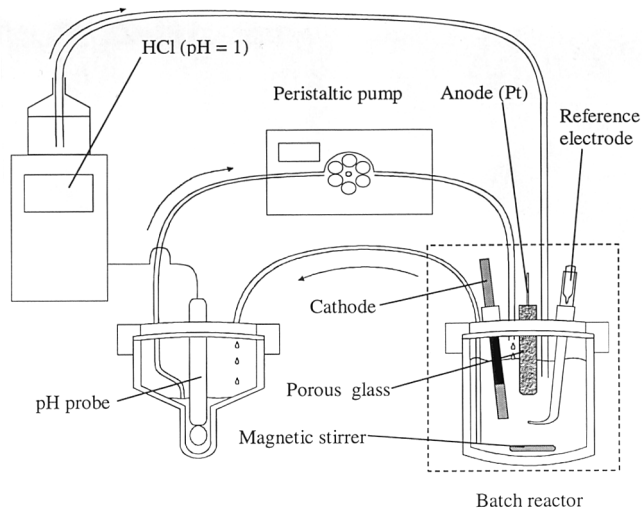

Fig. 3. Experimental setup.

in order to exclude interference of the cathodic metal deposition with chlorine evolved at the anode. Convection was achieved by a magnetic stirrer (IKA COMBIMAG RET, 500 RPM, magnet 15×5 min). The pH was measured continuously in a separate reservoir by using a peristaltic pump to transport the solution from the batch reactor to the reservoir and back. This separation was necessary to avoid interference of the pH measurement with the electric field resulting from the electrodeposition current. In addition, the pH was controlled by periodic additions of HCl (pH 1) (Metrohm Titrino 719S), which was necessary if the cell was operated at pH 3.5.

To investigate the feasibility of electrochemical separation from mixed solution of heavy metals, a graphite electrode was used. After changing the electrode potential, the current was allowed to stabilise for 10–20 s before recording the value.

For selective electrodeposition of the different metals, the cathode consisted of the respective metals of at least 99.9% purity. The use of identical cathode materials prevented problems such as nucleation. In order to have similar reduction conditions, such as surface growth and deposition time, the size of the cathode area used was adapted to the concentrations of the heavy metals in solution leading to related ratios of concentration to surface. For copper, it was 6.4×10^{-4} m^2, for lead 3.6×10^{-4} m^2, for cadmium 2.9×10^{-4} m^2 and for zinc 2.5×10^{-3} m^2. It has to be noted that the remaining differences of the ratios are due to geometrical problems imposed by the high surface differences and the variably shapes of the metals available. The main importance of this reactor, however, is not affected by these differences. The deposits were dried in an exsiccator using P_2O_5.

The rotating disc electrode method (RDE) as steady state technique was used to obtain information about the rate determining step (r.d.s) and the relevant parameters. The RDE material (EG&E Parc Model 616 rde) consisted of one of the four heavy metals. Only short current pulses were applied to prevent significant changes of surface roughness due to crystal growth. After each potential sweep at the same rotation speed, the electrode was cleaned by chemical etching with HNO_3, subsequent polishing using Al_2O_3 powder and rinsing with deionised water. The RDE cathodes were used for potential step (chronoamperometry) measurements as well. This method was used to confirm the data obtained with RDE measurements.

Heavy metal concentrations in the solution during the electrodeposition were determined using voltamperometry (Metrohm 646 VA processor). By dissolving the deposits in HNO_3, their purity was analysed by voltammetry as well (checking for the four different heavy metals and chlorides). ICP-AES (Varian Liberty) was used to analyse the composition of the Deglor secondary fly ash and to confirm some of the voltamperometric results. Ion chromatography was used to analyse the existing anions.

To study the deposits, a scanning electron microscope (SEM) JEOL JSM-6300 F was used. In addition, EDS measurements could be carried out to investigate the composition of different particles. For determining the specific surface, BET measurements (Sorptomatic 1990) with N_2 at 150°C were carried out.

3. Results and discussion

3.1. Feasible potential ranges for selective electrodeposition

Fig. 4 shows the quasi stationary voltammogram of the standard solution obtained with a graphite cathode. This figure shows the presence of five more or less well expressed current steps.

The first step between 0.4 and -0.32 V SCE corresponds to the reduction of Cu(II) to Cu(I) in Eq. (1), the second step in the potential region between around -0.33 and -0.58 V is caused by the reduction of Cu(I) to metallic Cu in Eq. (2).

$$Cu(II) + e \rightleftharpoons Cu(I) \quad (1)$$

$$Cu(I) + e \rightleftharpoons Cu \quad (2)$$

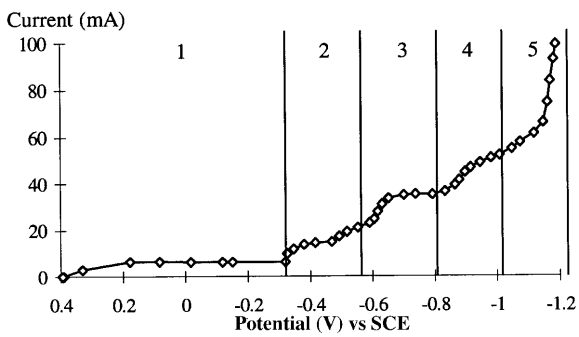

Fig. 4. Voltammogram for the synthetic solution A (pH 1.5). Each point was measured after having obtained a steady state. 1, Cu(II)/Cu(I) reduction; 2, Cu(I)/Cu(0) reduction; 3, Pb(II)/Pb(0) reduction; 4, Cd(II)/Cd(0) reduction; 5, Zn(II)/Zn(0) reduction and H^+ discharge.

The complexation of Cu(I) with the chloride evokes a stabilisation of the monovalent form and therefore two separated current steps occur.

Step 3 (from around -0.59 to -0.82 V) and 4 (from around -0.83 to -1.04 V) are due to the reduction of Pb(II) in Eq. (3)) and Cd(II) in Eq. (4), respectively.

$$Pb(II) + 2e \rightleftharpoons Pb \quad (3)$$

$$Cd(II) + 2e \rightleftharpoons Cd \quad (4)$$

The last step (above -1.05 V) is the reduction of Zn(II) in Eq. (5) with important simultaneous H_2 evolution in Eq. (6).

$$Zn(II) + 2e \rightleftharpoons Zn \quad (5)$$

$$H^+ + e \rightleftharpoons 0.5H_2 \quad (6)$$

These results show the feasibility of the selective deposition of each metal from the synthetic solution. For certain metal combinations, e.g. Me1 = Pb and Me2 = Cd, deposition of monolayer amounts in the potential range positive of the equilibrium potential, the so called under-potential deposition (UPD) [12], is possible. Ref. [13] shows a complete list of metal combinations, for which UPD has been found. For porous deposits, a monolayer of a foreign element may cause an important impurity as can be estimated for a Cd monolayer on Pb. BET measurements of the deposits reveal a specific surface area of, e.g. around 50 m^2/g for the Pb deposit at high overpotentials. A complete Cd monolayer of 1×10^{19} Atoms/m^2 on such a Pb deposit would lead to an impurity of around 6 mass% and 10 mol%, respectively. For Pb on Cu, where the specific surface of Cu is around 6 m^2/g, a lead impurity of 1.2 mass% and 0.4 mol%, respectively, can be estimated. In conclusion, UPD effects on deposit purity cannot be excluded.

Focussing on high deposition rates and purities, the useful potential ranges get smaller. In order to achieve realistic deposition currents, the overpotential should exceed a certain value, depending on n_{Me}, the number of electrons used for the reaction (see Section 3.2). At the negative end of the potential range, the above-mentioned UPD effects are limiting. In addition, simultaneous H^+ discharge, visible for the Zn and Cd reduction in Fig. 4, hide the equilibrium potential due to a superposition of an additional current and a resulting mixed potential. This makes the determination of a clear separation line difficult. This problem will be discussed in Section 3.6.

3.2. Achievable deposition rates

Tests with rotating disc electrodes showed in all cases, within the concentration range of interest, that the transport of mass is the rate limiting factor. The

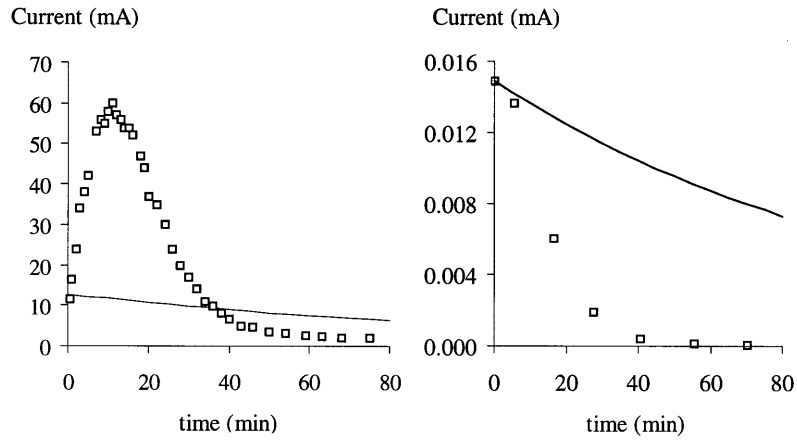

Fig. 5. Typical current/time (5 left) and concentration/time (5 right) transients (□, experiments; —, theory according to Eqs. (7) and (8)).

current during deposition for the metal Me can be expressed by the following formula:

$$i_{d,Me} = -n_{Me} \cdot F \cdot k_{Me} \cdot (a_{Me}^{z+} - a_{Me}^{z+0}) \cdot S_{Me} \quad (7)$$

Supposing constant agitation, i.e. a constant mass transfer coefficient k_{Me}, ($k_{Me} = D_{me}/\delta_{Me}$), only the heavy metal activity on the surface a_{Me}^{z+0} and the electro-active surface area S_{Me} influence the current. The activity a_{Me}^{z+0} is directly related to the applied potential according to Nernst, the electro-active surface area is a function of deposition time and depends on the deposit morphology.

Applying a sufficiently high overpotential leads to an a_{Me}^{z+0} near to 0 and maximises the rate (limiting current). As an example, for a reaction with $n_{Me} = 2$, an overpotential of around -50 mV leads, according to the Nernst equation, to an a_{Me}^{z+0} of 2% of the bulk activity a_{Me}^{z+}.

S_{Me} depends on the form of the deposited metal. The characteristic growth morphology changes, with increasing overpotential, from well formed layers, spirals or blocks to bunched layers and ridges. Near the limiting current, nodules and dendrites start to appear. Further increasing of the overpotential leads to powdery structure [14]. The texture type of the deposits is a function of several parameters such as cation sort and concentration, cathode type, agitation, temperature, current density, overpotential and anions [13]. In the first seconds of the electrodeposition, however, S_{Me} is known (geometric surface) and k_{Me} as only unknown parameters can be calculated for all electrodepositions.

According to this information, working near or at the limiting current, produces highly porous dendritic deposits, which leads to increasing S_{Me} and hence current in the initial phase of the deposition process. The current decreases later due to the diminishing concentration in solution, resulting in a current peak. Fig. 5 (left and right) illustrates a typical current/time and concentration/time transient in a case with dendritic metal growth. For comparison, the corresponding transients in the case of very dense deposits are illustrated. For a batch reactor, assuming constant S_{Me} and $a^{z+}{}_{0Me} = 0$, the theoretical activity decrease as function of the time t_{Me}^{th}, t is

$$a_{Me1}^{z+} = a_{Me\,ini}^{z+} \exp\left(-\frac{S_{Me} \cdot k_{Me} \cdot t_{Me}^{th}}{V}\right) \quad (8)$$

Replacing a_{Me}^{z+} of Eq. (7) by this result, the corresponding current transient is obtained.

For each heavy metal, the deposition rate enhancement due to growth of S_{Me} compared with a constant S_{Me}, according to Eq. (8) can now be described. Fixing a bulk concentration (5% of the initial amount), which has to be achieved, the ratio of time to comply this demand leads to the rate enhancement factor r_{Me} (t_{Me}^{exp} = experimental time, t_{Me}^{th} = theoretical time according to Eq. (8)).

$$r_{Me} = \frac{t_{Me}^{th}}{t_{Me}^{exp}} \quad (9)$$

The goal is to investigate the dependence of increasing S_{Me} on pH and overpotential. In addition, the best deposition conditions for of each heavy metal are compared in a separate chapter.

3.3. Reduction of copper

The reduction of Cu(II) occurs via two consecutive electron transfer reactions with Cu(I) as intermediate product [15]. The stability of Cu(I) depends on the anions in the electrolyte. In non-complexing solutions such as perchlorate, nitrate or sulfate, Cu(I) is not stable [16]. The standard reduction potential of Cu(I) to Cu(0) is higher than that of Cu(II) to Cu(I). Complexa-

tion with Cl^- stabilises Cu(I) leading to a higher value for the reduction potential of the redox reaction Cu(II)/Cu(I) than for the deposition potential of Cu(I). This explains the two waves appearing in the voltammogram in Fig. 4. $CuCl_2$ is easily soluble in water, whereas CuCl is hardly soluble.

The reduction of copper was carried out at -450 and -500 mV using solution A at pH 1.5. Before the electrodeposition was started, the mixed potential of the system Cu(II)/Cu(I)/Cu(0) (Eqs. (1) and (2)) was measured at open circuit. The value of -230 mV, obtained without agitation, was almost 100 mV higher than expected from Fig. 4. This difference can be explained by the overpotential necessary for the nucleation of Cu on graphite. Using this mixed potential as a reference, the corresponding overpotential η becomes -220 and -270 mV. The deposit density is lower at -170 mV, which is visible by the lower deposit volume and by SEM photographs as well. During the electrodeposition, Cu(I) is produced. The appearance of Cu(I) does not, however, influence the current efficiency for the overall reduction process [17].

The purity of the deposit is 99.8 mol% for $\eta = -220$ mV and 99.5 mol% for $\eta = -270$ mV, respectively. The main impurity was lead. Because of a large UPD-shift of Pb^{2+}, on Cu (around 130 mV in 0.5 M KCl), both overpotentials are within the UPD-range. The smaller the specific surface, the lower should be the deposited amount of Pb per mass unit of Cu, which would qualitatively explain the different purities. The calculation of 3.1 shows a very good agreement with the experimental results. Cd can also form a UPD layer on Cu, but its UPD-shift (230 mV in 1 M Na_2SO_4) is not large enough to interfere. This agrees with the experiments, where no Cd impurities were detected.

Concerning the rate enhancement r_{Cu} during the electrodeposition, the values are 2.8 for $\eta = -220$ mV and 3.3 for $\eta = -270$ mV, respectively.

The current efficiency is near 100%. Only the simultaneous reduction of dissolved O_2 was observed as a side reaction interfering at low Cu concentrations.

3.4. Reduction of lead

In the case of Pb, the reduction proceeds via a two electron mechanism. The high concentration of Cl^- increases the solubility of $PbCl_2$. Tests were carried out using two different values of pH. The applied potential was between -650 and -800 mV. Using the equilibrium potential of around -570 mV for the solution B (pH 1.5 or 3.5), measured at open circuit in the beginning of the reaction, this corresponds to an overpotential between -80 and -230 mV. For pH 3.5, overpotentials of -170 and -230 mV were applied.

The purity of Pb deposits was always above 99.8 mol%. The high purity might be due to the very small UPD potential shift for Cd on Pb.

The rate enhancement factor r_{Pb} shows values of more than 7 for the highest overpotential and it decrease to around 4 for the lowest. SEM photographs show well-developed ridges for -80 mV. With increasing overpotential, the form becomes more porous and less well formed with nodules and dendrites as growth mode, leading to very low densities. Therefore, the decrease of the rate enhancement factor with smaller overpotential directly correlates with the change of morphology. No significant structure difference with changing pH could be detected.

Neither important decrease of the current efficiency by H^+ discharge nor by O_2 reduction as side reactions was observed.

3.5. Reduction of cadmium

Deposition experiments were carried out at four potentials (-880, -920, -960 and -1020 mV) and two different values of pH. With an equilibrium potential at around -830 mV at open circuit for the solution C (pH 1.5 or 3.5), the applied overpotentials correspond to $\eta = -50$, -90, -130 and -190 mV.

The deposit purities for the highest overpotential at pH 3.5 was around 95 mol% and for pH 1.5 around 97 mol%. Lower η increased the purity, around 98 mol% for $\eta = -130$ mV and 99.2 mol% for $\eta = -90$ mV at pH 1.5. The literature [13] does not mention the existence of underpotential deposition of Zn on Cd. The potential range for selective Cd deposition seems to be restricted by the presence of Zn in a 10-fold excess.

Interesting is the development of the rate enhancement factor. For the highest overpotential, independent on the pH, r was around 7, which is significantly lower than the values obtained at -130 and -90 mV (with r around 9–10). The lowest overpotential shows values around 2. SEM photographs show a similar structure development with 11 as already found with Pb. Low η values lead to well formed and dense deposits. With increasing η, these change to long dendrites with diameters around 1 μm, which leads to very porous structures and low densities. For $\eta = -190$ mV, the dendrites become much more roughened and EDS measurements reveal crystals consisting of pure Zn in the case of pH 3.5. The deposition of pure bulk Zn proves that a potential below the Nernstian potential for deposition of Zn^{2+}, on Zn was reached. The depression of r, however, can not be explained by the codeposition of Zn since tests carried out under identical conditions but using a synthetic solution C without Zn reveal similar results. No Zn crystals could be found in deposits formed at pH 1.5.

Except for the highest overpotential, at pH 1.5, the current efficiency is high due to low H^+ discharge. No O_2 reduction was detected.

Table 2
Comparison of the enhancement factor of the four different heavy metals at optimal conditions

Heavy metal	Optimal deposition conditions		Enhancement factor r
	η (mV)	pH	
Cu	−270	1.5	3.3
Pb	−230	1.5 and 3.5	7.5
Cd	−90/−130	1.5 and 3.5	9
Zn	−330	3.5	2.5

3.6. Reduction of zinc

Even at pH 3.5, zinc corrosion leads to the establishment of a mixed potential. Hence, a well-defined equilibrium potential does not exist. A zinc electrode in a solution D (pH 3.5, open circuit) reveals a value of −1080 mV but the results from the previous section suggest values above −1020 mV. For practical reasons, −1080 mV is used as equilibrium potential to express the overpotentials. Deposition potentials at three potentials 1200, −1300 and −1400 mV), at pH 3.5, were carried out, corresponding to $\eta = -120$, −220 and −330 mV. The reduction of Zn at pH 1.5, visible in Fig. 4, is accompanied by a high rate of H^+ reduction. Therefore, no further measurements were carried out at this low pH.

No other metals considered in this study limit the applicable overpotential. Therefore, only the deposition time and yield must be optimised.

The SEM photographs for Zn reveal a very compact morphology, well attached to the electrode and not changing with η. Little surface increase can be expected during electroreduction. In addition, calculating a k_{Zn}, from the values of the current at the onset yields values which are around 5–6 times higher than those obtained for the other metals. It was observed that not the whole electrode area was covered by the deposit after electrodeposition which might explain this phenomenon. Possibly the ratio of the electrode surface to the electrolyte volume was too high, which resulted in areas of the electrode only in contact with the unstirred solution. As mentioned before, RDE and chronoamperometry measurements showed mass transfer as r.d.s. The r_{Zn} obtained, using the high value obtained for k_{Zn}, becomes maximal for $\eta = -320$ with r_{Zn} at around 3.

The deposition current efficiency is only slightly dependent on η, hence a technical deposition process will be optimised to run on high η.

3.7. Comparison of the four different metals

In order to compare the results of the four different metals, the optimum results of each metal are listed in Table 2. In addition, the SEM photographs are given for these four different results in Fig. 6.

As expected, Pb and Cd, the metals with the highest porosity and lowest deposit density, show also the highest r and therefore the highest deposition rate, whereas Zn is much slower due to the compact deposit structure, but also due to the experimental problems mentioned. Cu, which has an intermediate density, shows an intermediate deposition rate as well.

4. Conclusions

It has been shown that the selective electrodeposition of the four heavy metals Cu, Pb, Cd and Zn in purities above 99mol% is possible using potentiostatic conditions. The purities of Cu and Pb are higher or equal to 99.5 mol%. Cd must be deposited at lower overpotentials to prevent important Zn deposition, but purities around 99 mol% can be achieved as well. For Cu, Pb and Cd an optimum of deposit purity, current efficiency and time, even at low pH of 1.5, can be achieved by optimisation of the applied overpotential. The high chloride concentration shifts the equilibrium potential to the negative, but does not cause severe problems, such as decreasing the deposition rate during electrodeposition. Using high overpotentials increases the available electroactive surface due to dendritic growth,

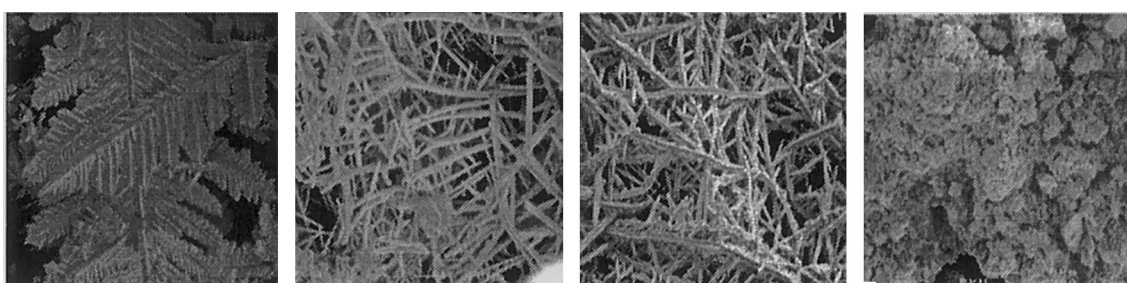

Fig. 6. Scanning electron microscope (SEM) photography for the deposit of the best results (From left to right: Cu, Pb, Cd and Zn, size 80 × 80 μm).

which leads to a high enhancement factor and thus minimises the time needed for electrodeposition. In general, the lower the deposit density, the higher becomes the deposition rate. Therefore, Pb and Cd show the highest enhancement factor, Zn the lowest and Cu an intermediate value. Except for Zn, the deposits adhere poorly to the surface. Thus, the deposit can be removed without removing the cathode. Further experiments using a bench scale reactor will show if the process with similar purities can be carried out technically and will give information for estimating the costs of such a process.

Appendix A. Nomenclature

$a^{z+}_{\mathrm{Me\ ini}}$	bulk activity of the Me ion with charge z (or atom, when $z=0$) in the beginning
a^{z+}_{Me}	bulk acitivity of the Me ion with charge z (or atom, when $z=0$)
a^{z+0}_{Me}	surface activity of the Me ion with charge z (or atom, when $z=0$)
D_{Me}	diffusion coefficient of the Me ion, m^2/s
δ_{Me}	Nernstian diffusion layer, m
F	Faraday constant, 96 485 C/mol
$i_{\mathrm{d,Me}}$	diffusion limited current for the metal Me, A
k_{Me}	mass transfer coefficient, m/s
n_{Me}	number of electrons involved in overall electrode reaction
r_{Me}	rate enhancement factor
S_{Me}	total active surface, m^2
$t^{\mathrm{exp}}_{\mathrm{Me}}$	experimental time for a reduction, s
$t^{\mathrm{th}}_{\mathrm{Me}}$	theoretical time for a reduction, s
V	volume of the solution, m^3

References

[1] J.A. Harrison, Electrochim. Acta 24 (1979) 179.
[2] A. Fontana, J. van Muylder, R. Winand, Electrochim. Acta 30 (1985) 641.
[3] D.R. Jovanovic, T. Rakic, Electrochim. Acta 22 (1977) 233.
[4] W.C. Hsie, M.L. Gopikanth, J.R. Selman, Electrochim. Acta 30 (1985) 1371.
[5] W.C. Hsie, J.R. Selman, Electrochim. Acta 30 (1985) 1381.
[6] E. Skou, T. Jacobsen, W. Van der Hoeven, S. Atlung, Electrochim. Acta 22 (1977) 169–174.
[7] R. Suzuki, W.-H. Li, M. Schwartz, K. Nobe, Plat. Surf. Finish, 58 (1995).
[8] J. Wang, H. Dewald, J. Electrochem. Soc. 130 (1814) 1983.
[9] R.D. Armstrong, M. Todd, J.W. Atkinson, K. Scott, J. Appl. 27 (1997) 965.
[10] A. Jakob, S. Stucki, P. Kuhn, Environ. Sci. Technol. 29 (1995) 2429.
[11] J. Balg, C. Wieckert, ABB Technik, 9 (5/6) (1995).
[12] D.M. Kolb, in: H. Gerischer (Ed.), Advances in Electrochemistry and Electrochemical Engineering, vol. 11, Wiley, New York, 1978, p. 446.
[13] E. Budevski, G. Staikov, W.J. Lorenz, in: D.M. Bär (Ed.), Electrochemical Phase Formation and Growth, VCH, Weinheim, 1996, p. 410.
[14] D. Pletcher, C. Walsh, in: D. Pletcher (Ed.), Industrial Electrochemistry, Chapman and Hall, New York, 1990, p. 399.
[15] U. Bertocci, Electrochim. Acta 11 (1966) 1261.
[16] U. Bertocci, D.R. Turner, in: A.J. Bard (Ed.), Copper, vol. 2, Marcel Dekker, New York, 1973, p. 383.
[17] L. Doulakas, S. Stucki, C. Comninellis, in: E.J. Rud, C.W. Walton (Eds.), Enegrie and Electrochemical Processing for a Cleaner Environment, vols. 97–28, The Electrochemical Society Proceedings Series, Pennington, NJ, 1997, p. 331.